Electrokinetic measurements of membrane capacitance and conductance for pancreatic β-cells

R. Pethig, L. Jakubek, R.H. Sanger, E. Heart, E. Corson and P.J.S. Smith

Abstract: Membrane capacitance and membrane conductance values are reported for insulin secreting cells (primary β-cells and INS-1 insulinoma cells) determined using the methods of dielectrophoresis and electrorotation. The membrane capacitance value of 12.57 (± 1.46) mF/m^2 obtained for β-cells, and the values 9.96 (± 1.89) mF/m^2 to 10.65 (± 2.1) mF/m^2 obtained for INS-1 cells, fall within the range expected for mammalian cells. The electrorotation results for the INS-1 cells lead to a value of 36 (± 22) S/m^2 for the membrane conductance associated with ion channels, if values in the range 2nS to 3 nS are assumed for the membrane surface conductance. This membrane conductance value falls within the range reported for INS cells obtained using the whole-cell patch-clamp technique. However, the total 'effective' membrane conductance value of 601 (± 182) S/m^2 obtained for the INS-1 cells by dielectrophoresis is significantly larger (by a factor of around three-fold) than the values obtained by electrorotation. This could result from an increased membrane surface conductance, or increased passive conduction of ions through membrane pores, induced by the larger electric field stresses experienced by cells in the dielectrophoresis experiments.

R. Pethig is with the School of Informatics, University of Wales, Bangor, Gwynedd, LL57 1UT, UK

R. Pethig, L. Jakubek, R.H. Sanger, E. Heart, E. Corson and P.J.S. Smith are with the BioCurrents Research Center, Program in Molecular Physiology, Marine Biological Laboratory, Woods Hole, MA 02543, USA

L. Jakubek is with the Dept. of Molecular and Cell Biology, Brown University, Providence, R.I., USA

E-mail: ron@informatics.bangor.ac.uk; psmith@mbl.edu

1. Introduction

In this paper we report determinations of the membrane capacitance and membrane conductance for insulin secreting cells, both rat derived insulinoma cells and mouse primary β-cell cultures, using the electrokinetic techniques of dielectrophoresis (DEP) and electrorotation (ER). These methods avoid the need to make electrode contact to the cells, and many cells can be investigated at the same time for a range of physico-chemical environments. The magnitude of the membrane capacitance can be taken as a measure of the total surface area of the cell, and the extent to which this is enhanced by membrane features such as blebs and microvilli, for example. The membrane conductance comprises two main components, namely the conductance across the membrane associated with ion flux through membrane pores and ion channels, together with ionic conduction parallel to the membrane surface associated with the electrical double-layer induced by the net negative charge carried by all cells.

Like neurons and muscle cells pancreatic β-cells are excitable displaying calcium dependent action potentials in bursting patterns. This activity is a key component of glucose responsive insulin release, exhibiting a hierarchal order of control such that isolated cells [1], islets (for rat see [2]) and insulin blood levels [3] all exhibit a cyclic pulsatile behaviour. To advance our understanding of normal insulin release and diabetes we need to generate good models for insulin release at the single cell level and build from there. For this study, therefore, the pancreatic β-cell, and immortal insulinoma cell lines offer key advantages. Firstly, there exists information on the electrical behaviour of these cells, metabolic control and vesicle fusion events [4,5]. Secondly, the disease relevance gives any methodology that allows large scale observation and modeling of capacitance and conductance – attributes that change in response to glucose stimulation – clear applications in both the basic biology of insulin release and in the screening of novel pharmacological or therapeutic compounds.

The theoretical and experimental aspects of DEP and ER are well described in the literature [6-10]. In brief, when a cell is exposed to an electrical field it becomes electrically polarized. This polarization takes the form of induced charges that are generated at the cell's external surface, and also within the cell at interfaces between the cytoplasm and the plasma membrane, endoplasmic reticulum and nucleus, for example. The distribution of these charges produces a macroscopic dipole moment, whose magnitude and polarity depends on

the dielectric properties of the surrounding solution, as well as those of the various components of the cell. If an alternating current (a.c.) field is applied at a particular frequency, the induced dipole moment will lag the field by a phase angle whose value depends on the dielectric properties of the cell and the solution at that frequency. For the frequency range (10 kHz - 10 MHz) and solution conductivities (10 - 100 mS/m) used in this work, the polarizability of a viable cell is largely determined by the resistance and capacitance of the plasma membrane, and the lagging phase angle has a value greater than 180^{o}. If the a.c. field is highly non-uniform the cell will move under the influence of a DEP force. At the lower frequencies, and for the solution conductivities used in our experiments, a viable cell will exhibit negative DEP and be repelled from electrode edges. At the higher frequencies the cell will be attracted to the electrodes by positive DEP. If the a.c. field is rotated, the cell will experience a rotational torque and rotate in an anti-field sense over most of the frequency range between 10 kHz and 10 MHz. Values for the membrane capacitance and conductance are obtained by determining the frequency where the antifield rotation rate reaches its maximum value, and the frequency at which the DEP response makes the transition from negative to positive DEP.

2. Theory

A cell of radius r, when exposed to a rotating electric field in a solution of conductivity σ_s, will exhibit a maximum antifield ER rate at a frequency f_{pk} given by [7]:

$$f_{pk} = \frac{K_{ms}}{\pi r^2 C_m} + \frac{G_m}{2\pi C_m} + \frac{\sigma_s}{\pi r C_m} \qquad (1)$$

This relationship holds for the case where the conductivity σ_s of the external solution is much lower than the internal conductivity of the cell. This condition was met in our experiments. In equation (1) C_m and G_m are the trans-membrane capacitance and conductance values, respectively, and K_{ms} is the surface conductance of the cell membrane. Values for C_m for mammalian cells (e.g., erythrocytes, monocytes, granulocytes, B and T cells) range from around 10 to 15 mF/m^2 [10], whilst G_m values associated with ion channel conduction typically range from around 10 to 100 S/m^2 [11]. Values for K_{ms} have been assumed to be similar to those for cell-sized polystyrene particles (0.2 to 2 nS) and to be independent of the solution conductivity and field frequencies between 100 kHz and 1 MHz [7].

To accommodate the fact that in our experiments the cells exhibited a range of radii, values of $f_{pk}.r$ for various solution conductivities were recorded. From equation (1) we expect a plot of $f_{pk}.r$ against σ_s to be linear (of the form y = *m*x + *c*) and have a slope *m* given by

$$m = \frac{1}{\pi C_m} \tag{2}$$

and an intercept *c* given by

$$c = \frac{1}{\pi C_m}\left(\frac{K_{ms}}{r} + \frac{rG_m}{2}\right) = \frac{r}{2\pi C_m}\left(\frac{2K_{ms}}{r^2} + G_m\right) \tag{3}$$

Huang *et al* [12] have derived an expression for the DEP cross-over frequency f_{xo}, and by re-arranging the terms in their equation we obtain:

$$f_{xo} = \frac{\sqrt{2}\,\sigma_s}{2\pi r C_m}\sqrt{1 - \frac{rG_m^*}{2\sigma_s} - 2\left(\frac{rG_m^*}{2\sigma_s}\right)^2} \tag{4}$$

Although not formally stated in the earlier work [12], G_m^* should be taken as the total 'effective' membrane conductance, which from equation (3) can be given as:

$$G_m^* = \left(\frac{2K_{ms}}{r^2} + G_m\right) \tag{5}$$

For the DEP experiments reported here, the average value for *r* was around 5 μm, and values for σ_s ranged from 49 to 101 mS/m. For $G_m \le 600$ S/m^2 the factor $\frac{rG_m^*}{2\sigma_s}$ should not exceed a value of 0.03, so that (on simple application of the Binomial Theorem) to a very good approximation equation (4) can be simplified to the form:

$$f_{xo} \cdot r = \frac{\sqrt{2}}{2\pi C_m}\sigma_s - \frac{\sqrt{2}\,G_m^* r}{8\pi C_m} \tag{6}$$

From equation (6) we expect a plot of $f_{xo}.r$ against σ_s to be linear and have a slope *m* given by:

$$m = \frac{\sqrt{2}}{2\pi C_m} \tag{7}$$

and an intercept *c* given by:

$$c = -\frac{\sqrt{2}\, G_m^* r}{8\pi C_m} \tag{8}$$

3. Experimental

3.1 Cell Samples

INS-1 (rat insulinoma β-cells) were cultured using standard procedures [13] summarized here. The cells were grown in RPMI 1640 medium (Invitrogen) supplemented with 10 mM HEPES, 10% heat-inactivated fetal calf serum, 2 mM L-glutamine, 1 mM sodium pyruvate, 50 μM β-mercaptoethanol, and 100U/ml penicillin–streptomycin. A humidified incubator was used and maintained at 37°C with 5% CO_2, 95% air. Immediately before the experiments, the cells were centrifuged and washed twice in the media to be used in the DEP and ER measurements (see below)

Pancreatic islets were isolated from Swiss-Webster mice (Charles River) by collagenase digestion as previously described [14]. Briefly, following CO_2 asphyxiation, 2 ml of ice-cold collagenase (0.5 mg/ml, Roche) was infused into the common bile duct. The inflated pancreas was dissected and incubated for 10 minute at 37ºC, followed by vigorous shaking. After three washes, islets were picked by hand four times under a dissecting microscope and after overnight culture dispersed by incubation in Ca^{2+}/Mg^{2+} free PBS containing 3 mM EGTA and 0.05 mg/ml trypsin for 10 minutes at 37°C with occasional agitation. Immediately before the experiments, isolated islet cells were centrifuged, washed and suspended in the DEP and ER solutions.

3.2 DEP and ER Solutions

Cell suspending solutions of physiological osmolarity were prepared to cover the conductivity range from 11.5 to 101.4 mS/m at 22.5 °C. For the range 11.5 to 42.5 mS/m, the solutions contained 2mM glucose, 5.5 mM Hepes buffer, and adjusted to 300 mos by adding

96 g/mL sucrose. The pH was adjusted to pH 7.4 using NaOH, and the conductivity of individual aliquots was adjusted using KCl. For the range 48.7 to 101.4 mS/m, a stock solution was prepared, comprising: 140 mM NaCl; 5.4 mM KCl; 2.5 mM $CaCl_2$; 0.5 mM $MgCl_2$; 11 mM glucose and 5.5 mM Hepes buffer. The solution of highest conductivity (101.4 mS/m) was prepared by adding 8 mL of this stock solution to 92 mL double-distilled water, plus 8.47 g sucrose to give 300 mos. Lower conductivities were prepared through higher dilutions of the stock solution and a higher concentration of sucrose to achieve 300 mos. The conductivities were measured, to within ± 0.25%, using a YSI 3200 Conductivity Instrument (probe constant K = 1.0/cm).

3.3 Electrokinetic Experiments

Gold microelectrodes were manufactured by photolithography in a class II clean room onto glass microscope slides, with a 5 nm chrome adhesion layer and a 70 nm gold layer. Two basic geometries were employed – namely quadrupolar electrodes of the polynomial [15] and 'bone' design [16]. These electrode geometries are shown in Figure 1.

Digitally generated voltages of frequencies between 10 kHz and10 MHz, produced using a custom-built generator, were applied to each quadrupole electrode in sequence through 75Ω coaxial cables. For the ER experiments the 'bone' design electrodes were energized with 8 V (pk-pk) signals in phase quadrature so that, as viewed down the microscope and on a TV monitor, the resultant field between the electrodes rotated in a clock-wise sense. For DEP experiments, voltage signals up to 10 V (pk-pk) were applied to the polynomial design electrodes and arranged to give 180^o phase difference between adjacent electrodes. The magnitudes and phases of the four electrode voltages were monitored with a Tektronix TDS3024B oscilloscope.

The electrode arrays were cleaned with alcohol and pure water, and then submerged in water for at least two hours before each experiment. The cells, at a working concentration of 2 x 10^5 cells/mL or lower, were pipetted directly onto the electrodes and secured with a cover slip. At this concentration most of the suspended cells remained apart during the electrokinetic experiments. The concentration of cells shown in Figure 1 is of the order 5 x 10^5 cells/mL, and at this concentration many cells have been attracted together as a result of

mutual dipole-dipole interactions. The islet cells exhibited a tendency to adhere quite quickly to the glass substrate, and to avoid this effect the electrodes were energized with a rotating field before adding the cells to the electrode array. The electrokinetic responses of the cells were visualized using a Zeiss Axioskop and recorded at 30 frames/sec for later analysis, with a final magnification of 750 on a TV monitor.

In the DEP measurements attention was focused on cells located about 10~20 μm away from an electrode edge, where the field gradient and resulting DEP force would be greater than for cells located further away from the electrodes. The applied voltage frequency was adjusted to cause the cell under examination to sequentially make transitions between positive and negative DEP. The DEP cross-over frequency f_{xo} was determined either by finding the frequency where the cell became stationary, or by interpolating the estimated cell velocities to find the frequency where the DEP force acting on the cell was zero. ER rates were obtained mainly by simple timing with a stopwatch. When better accuracy was required to determine the maximum rotation rate, the video-captured frames were analyzed using an image processing method described previously [17]. Measurements were not made for cells that had interacted to form doublet or higher-order 'pearl chain' formations. The exact distance between opposite electrode faces (e.g., 393 μm for the nominal 400 μm bone electrodes) was used as the scale to determine cell diameter to an accuracy of ± 0.3 μm.

4. Results

The dispersed pancreatic islet cells tended to adhere strongly to the glass substrate, so that relatively few successful rotation measurements could be obtained for any one cell over the complete frequency range from 10 kHz to 10 MHz. This, coupled with the relatively low number of cells that could be harvested, made it impractical to perform a statistically meaningful ER analysis across the full conductivity range offered by the prepared suspending solutions. The most extensive set of results were obtained using a solution conductivity of 60.3 mS/m, where complete anti-field rotation spectra and values for f_{pk} were obtained for a total of 17 islet cells. Examples of two of these ER spectra are shown in Figure 2. The membrane capacitance C_m was obtained for each cell using equation (1) and assumed values for K_{ms} and G_m of 2 nS and 100 S/m^2, respectively. The mean value obtained for C_m was 12.57 mF/m^2, with a standard deviation of 1.46 mF/m^2.

The ER results obtained for the INS-1 cells are shown in Table 1 and Figure 3. The straight lines and formulae shown in Figure 3 are the best linear regression plots obtained using the Microsoft Excel program. From equation (2), using the slope values of 0.0299 and 0.0311, membrane capacitance values of 10.65 mF/m^2 and 10.23 mF/m^2 are derived for the low and higher conductivity data ranges, respectively. The estimated standard deviation for both capacitance results is 2.1 mF/m^2. Based on these C_m values, the total membrane conductance G_m^* given by equation (5) can be evaluated using the intercept values given in Figure 3. The 70 cells examined with the lower range (11.5 - 42.5 mS/m) of solution conductivities were determined to have a radius of 5.3 (± 0.68) μm which, together with C_m = 10.65 (± 2.1) mF/m^2 and c = 0.0207, leads to a value for G_m^* of 261 (± 85) S/m^2. The corresponding value obtained for the higher range (48.7 - 101.4 mS/m) of solution conductivities, for which the 108 cells examined had an average radius of 5.28 (± 0.72) μm, c = 0.0147 and C_m = 10.23 (± 2.1) mF/m^2, is G_m^* = 179 (± 61) S/m^2.

The results obtained from the DEP cross-over frequency measurements on the INS-1 cells are shown in Table 2 and Figure 4. From equation (7), and based on the value (0.0226) for the slope of the linear plot in Figure 4, a value of 9.96 mF/m^2 is derived for the membrane capacitance. The estimated standard deviation is 1.89 mF/m^2. From equation (8), using the mean radius value of 5.3 (± 0.6 μm) determined for the 86 cells examined in the DEP experiments, a mean value of 601 (± 182) S/m^2 is obtained for the total effective membrane conductance G_m^*.

5 Discussion and Conclusions

These studies demonstrate that pancreatic β-cells can be characterized and manipulated using the techniques of dielectrophoresis and electrorotation. The dispersed islet cells, if allowed to settle after being loaded onto the electrode assembly, were found to quickly stick to the glass substrate surface. This effect was partially overcome by applying an ER signal to the electrodes during the initial loading of the islet cells. However, a better approach will be to chemically treat or coat the glass substrate to reduce cell adhesion, and this is currently being

investigated in our laboratories. The cultured INS-1 β-cells did not adhere to the glass substrate during the experiments and, because sufficient numbers of cells were obtained from the immortalized cell line, measurements could be made for nine different solution conductivities covering the range from 11 to 101 mS/m.

The membrane capacitance value of 12.57 ± 1.46 mF/m^2 obtained for islet cells, and those of 10.23 ± 2.1; 10.65 ± 2.1 mF/m^2 (ER measurements) and 9.96 ± 1.89 mF/m^2 (DEP measurements) obtained for INS-1 cells, fall within the range of values determined by ER for T-cells (10.5 ± 3.1 mF/m^2), B-cells (12.6 ± 3.5 mF/m^2) and granulocytes (11.0 ± 3.2 mF/m^2) [18]. The ER results for blood cells were obtained for a single suspending medium conductivity (56 mS/m) and were analyzed using the so-called 'single-shell model' for cell structure. The standard deviations obtained in our experiments (1.46 and 2.1 mF/m^2) are less than those (3-1 - 3.5 mF/m^2) reported [18] for blood cells, and this may reflect the fact that β-cells exhibit a smaller biological variability than blood cells in terms of their membrane morphology. Also, because these membrane capacitance values are less than half the value of 26 mF/m^2 determined for human breast cancer cells [19], we can conclude that β-cells in their resting state are relatively devoid of surface features such as blebs and microvilli, for example. We base these conclusions on the fact that membrane capacitance values correlate closely with the extent to which the area of an otherwise smooth membrane surface is increased as a result of the presence of membrane folds and protuberances [10, 12, 18,19].

The suspending solutions contained 2 mM glucose or less, and so the INS-1 cells would have been in their resting state. Potassium conductance across the membrane dominates in the resting state of insulin-secreting cells, especially that associated with the ATP-sensitive K^+ channels [20]. Whole-cell patch-clamp measurements on INS cells have produced values for this K_{ATP} conductance of 2,240 (± 248) pS/pF [20]. Based on the mean membrane capacitance value of 10.44 (± 2.1) mF/m^2 obtained in our work for the INS-1 cells, this leads to a G_m value for potassium conductance of 23 (± 7) S/m^2, assuming no contributions from other ion channels or pores. The G_m^* value derived for the INS-1 cells from the ER measurements at the high conductivity range is 179 (± 61) S/m^2, and it is of interest to note that if we assign a surface conductance K_{ms} value equal to the normally accepted upper value

of 2 nS [7], then from equation (5) we can determine the ion channel conductance G_m value to be 36 (± 22) S/m^2. This result lies within the range of the K_{ATP} conductance obtained from the patch-clamp work. However, the K_{ms} value would need to be increased to 3.3 nS for the G_m^* value of 261 S/m^2, obtained with the low conductivity solutions, to lead to a G_m value close to that of the K_{ATP} conductance value. In principle, the result from the low conductivity solutions should produce a more accurate determination for G_m based on the intercept value of the linear plot shown in Figure 3, but this can be balanced against the fact that a larger number of cells (108 against 70) were examined at the higher conductivity range.

Finally, a mean value of 601 (± 182) S/m^2 was obtained for the total membrane conductance G_m^* from the DEP cross-over frequency measurements for the INS-1 cells. Although this result is considerably larger than the values obtained from the ER measurements, it is similar to that of 567 (± 326) S/m^2 obtained for rat kidney cells using the same DEP method [12]. It is not clear why membrane conductance values obtained using the ER and DEP techniques should differ so greatly. One reason could be associated with the fact that as a deliberate strategy to maximize the sensitivity of the DEP cross-over experiments, the 'target' cells were those near (~ 20 μm and closer) to the electrodes. In this situation the cells would experience much larger DEP forces and field stresses than cells further away from the electrodes, and this is a particularly relevant consideration when operating at a field frequency close to the DEP cross-over frequency f_{xo} [21]. This, in turn, could lead to an increased passive conduction of ions through membrane pores and to increased conduction of ions over the cell membrane surface. In the ER measurements, the cells would experience a uniform rotating field and field stresses much lower than that for the cells characterized for their DEP behaviour. These aspects are now subject to further investigations in our laboratories. We have no evidence to suggest that our applied a.c. electric fields in any way influence ion channel conductances, but this possibility should also be considered.

6. Acknowledgements:

The INS-1 cells used in this study were a gift from Jude Deeney of the Boston University Medical Center. This study was financed by a gift from the Denis Robinson Memorial Fund to RP and NIH grants NCRR RR001395 and DK06984 to PJSS. We thank Mark Messerli

and Leon Collis for valuable discussions, and Robert Lewis and Craig Hamilton for their assistance.

7. References

1. Ashcroft, F.M., and Rorsman, P.: 'Electrophysiology of the pancreatic beta-cell', *Prog Biophys Mol Biol* 1989, **54(2)**, pp. 87-143

2. Ikeuchi, M., Fujimoto, W.Y., and Cook, D.L.: 'Rat islet cells have glucose-dependent periodic electrical activity', *Horm Metabol Res.,* 1984, **16**, pp. 125-127

3. Pørksen, N.: 'The in vivo regulation of pulsatile insulin secretion', *Diabetologia* 2002, **45**, pp: 3-20

4. Rutter, G.A.: 'Nutrient –secretion coupling in the pancreatic islet β-cell: recent advances', *Molecular Aspects of Medicine* 2001, **22**, pp. 247-284

5. Tarasov, A., Duschonet, J., and Ashcroft, F.: 'Metabolic regulation of pancreatic β-cell ATP-sensitive K^+ channel: a ps de deux', *Diabetes* 2004, **53**, pp. S113-122

6. Pohl, H.A.: 'Dielectrophoresis' (Cambridge University Press, Cambridge, 1978)

7. Arnold, W.M. and Zimmermann, U.: 'Electro-rotation: Development of a technique for dielectric measurements on individual cells and particles', *J. Electrostatics*, 1988, **21**, pp. 151-191

8. Jones, T.B.: 'Electromechanics of particles' (Cambridge University Press, Cambridge, 1995)

9. Morgan, H. and Green, N.G.: 'AC electrokinetics: colloids and nanoparticles' (Research Studies Press, Herts, UK, 2003)

10. Pethig, R.: 'Cell physiometry tools based on dielectrophoresis', in Ozkan, M. and Heller, M.J. (Eds): 'BioMEMS and biomedical nanotechnology', **II**, pp. 103-126 (Springer Science, New York, 2005)

11. Lewis, S.A., and Hanrahan, J.W.: in Poste, G., and Crooke, S.T. (Eds): 'New Insights into Cells and Membrane Transport Processes' (Plenum Press, New York) 1986, pp. 305-326

12. Huang, Y., Wang, X.B., Becker, F.F. and Gascoyne, P.R.C.: 'Membrane changes associated with the temperature-sensitive $P85^{gag\text{-}mos}$-dependent transformation of rat kidney cells as determined by dielectrophoresis and electrorotation', *Biochim. Biophys. Acta*, 1996, **1282**, pp. 76-84

13. Farfari, S., Schultz, V., Corkey, B.E., and Prentki, M.: 'Glucose-regulated anaplerosis and cataplerosis in pancreatic β-cells', *Diabetes* 2000, **49**, pp. 718-726

14. Larson, O., Deeney, T.J., Branstrom, R., Berggren, P.O., and Corkey, B.E.: 'Activation of the ATP-sensitive K^+ channel by long chain acyl-CoA: role in modulation of pancreatic beta-cell glucose sensitivity', *J Biol Chem* 1996, **271**, 10623-10626

15. Huang, Y., and Pethig, R.: 'Electrode design for negative dielectrophoresis', *Meas. Sci. Technol.,* 1991, **2**, pp. 1142-1146

16. Dalton, C., Goater, A.d., Drysdale, J., and Pethig, R.: 'Parasite viability by electrorotation', *Colloids and Surfaces A: Physicochem. Eng. Aspects*, 2001, 195, pp. 263-268

17. Zhou, X.F., Burt, J.P.H., and Pethig, R.: 'Automatic cell electrorotation measurements', *Phys. Med. Biol*., 1998, **43**, pp. 1075-1090

18. Yang, J., Huang, Y., Wang, X., Wang, X.B., Becker, F.F. and Gascoyne, P.R.C.: 'Dielectric properties of human leukocyte subpopulations determined by electrorotation as a cell separation criterion' *Biophys. J*., 1999, **76**, pp. 3307-3314

19. Becker, F.F., Wang, X.B., Huang, Y., Pethig, R., Vykoukal, J. and Gascoyne, P.R.C.: 'Separation of human breast cancer cells from blood by differential dielectric affinity' *Proc. Natl. Acad. Sci. USA*, 1995, **92**, pp. 860-864

20. Nakazaki, M., Kakei, M., and Ishihara, H., *et al*.: 'Association of unregulated activity of KATP channels with impaired insulin secretion in UCP1-expressing insulinoma cells' *J. Physiol*., 2002, **540.3**, pp. 781-789

21. Menachery, A., and Pethig, R.: 'Controlling cell destruction using dielectrophoretic forces' *IEE Proc. Nanobiotechnol*. 2005, 152, pp. 145 – 149

Figure Legends

Figure 1: The polynomial (left) and 'bone' (right) quadrupolar electrode designs used in the DEP and ER experiments, respectively. For DEP measurements, non-uniform electric fields were produced by energizing adjacent electrodes with a.c. signals phased 180^o apart. A rotating field was generated by energizing the electrodes with four signals, each separated by 90^o phase angle.

Figure 2: Electrorotation spectra obtained for two isolated pancreatic islet cells suspended in a solution of conductivity 60.3 mS/m, and with applied quadrature signals of 8 V (pk-pk).

Figure 3: Plots of the electrorotation data given in Table 1 for the INS-1 cells. The straight lines represent the best linear regression plots of the data obtained for the two sets of suspending media. The corresponding linear equations and correlation coefficient are presented.

Figure 4: Plot of the DEP cross-over data given in Table 2 for the INS-1 cells. The straight line, and corresponding linear equation providing the slope and intercept values, was used to derive a value of 9.96 (± 1.89) mF/m^2 and 600 (± 340) S/m^2 for the membrane capacitance C_m and effective membrane conductance G_m^*, respectively.

TABLES

Table 1: The data obtained from determination of cell radius and the frequency f_{pk}, defining the maximum anti-field electrorotation rate, for the INS-1 cells. The mean and standard deviation values are given for the cell radius r and the product f_{pk} .r for cells (number n) suspended in the two sets of suspending media used to cover the conductivity range from 11.5 to 101 mS/m.

Conductivity (mS/m)	Cells n	Radius r (μm)	f_{pk} .r (m/sec)
Range 1			
11.5	15	5.3 (0.76)	0.39 (0.10)
21.7	21	5.6 (0.84)	0.62 (0.14)
32.8	15	5.6 (0.54)	1.03 (0.22)
42.5	19	5.3 (0.63)	1.29 (0.30)
Range 2			
48.7	25	4.95 (0.67)	1.58 (0.40)
60.3	15	5.28 (0.77)	1.85 (0.43)
74.9	24	5.61 (0.70)	2.34 (0.67)
86.9	20	5.28 (0.67)	2.66 (0.54)
101.4	24	5.61 (0.71)	3.23 (0.66)

Table 2: The results obtained from determination of the DEP cross-over frequency f_{xo} for the INS-1 cells. The mean and standard deviation values are given for the cell radius r and the product f_{xo} .r for cells (number n) suspended in solutions of different conductivity.

Conductivity (mS/m)	Cells n	Radius r (μm)	f_{xo} .r (m/sec)
48.7	19	5.24 (0.45)	1.08 (0.26)
60.3	14	5.72 (0.86)	1.33 (0.21)
74.9	15	5.28 (0.70)	1.69 (0.38)
86.9	18	4.96 (0.68)	1.98 (0.47)
101.4	20	5.28 (0.63)	2.25 (0.43)

Figure 1

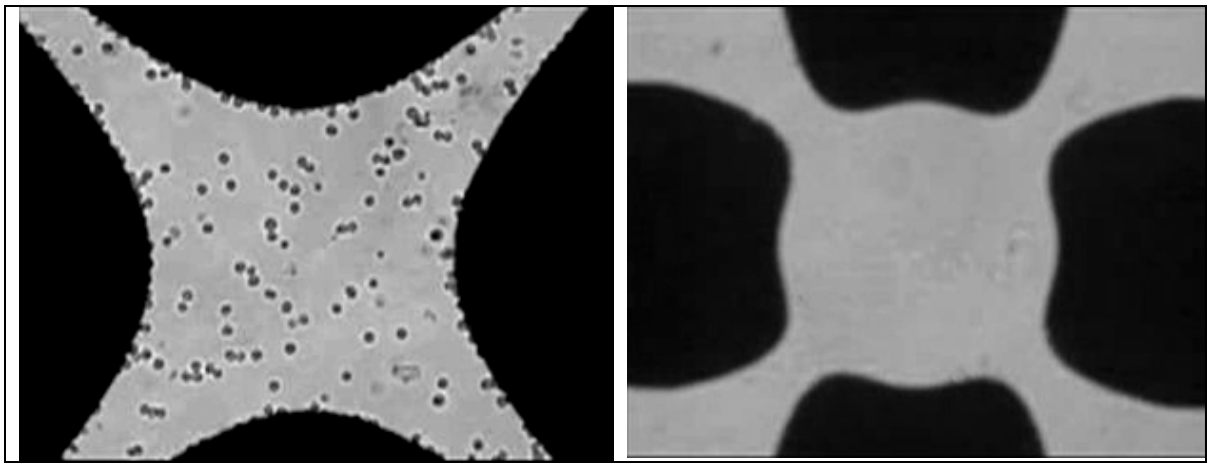

Figure 2

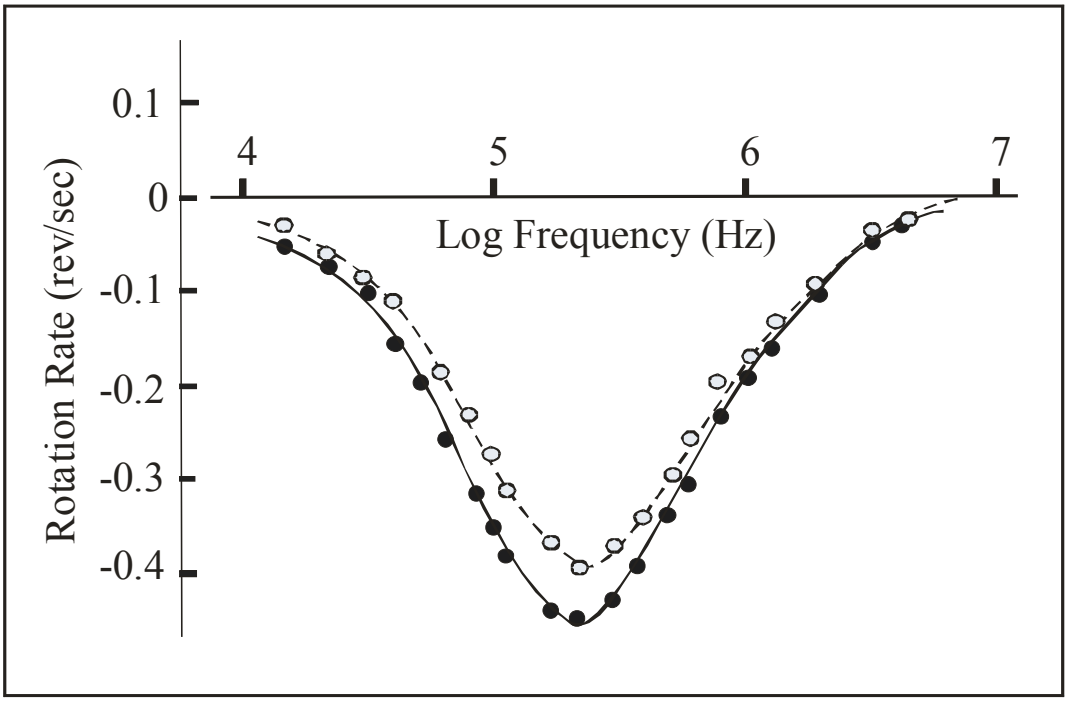

Figure 3

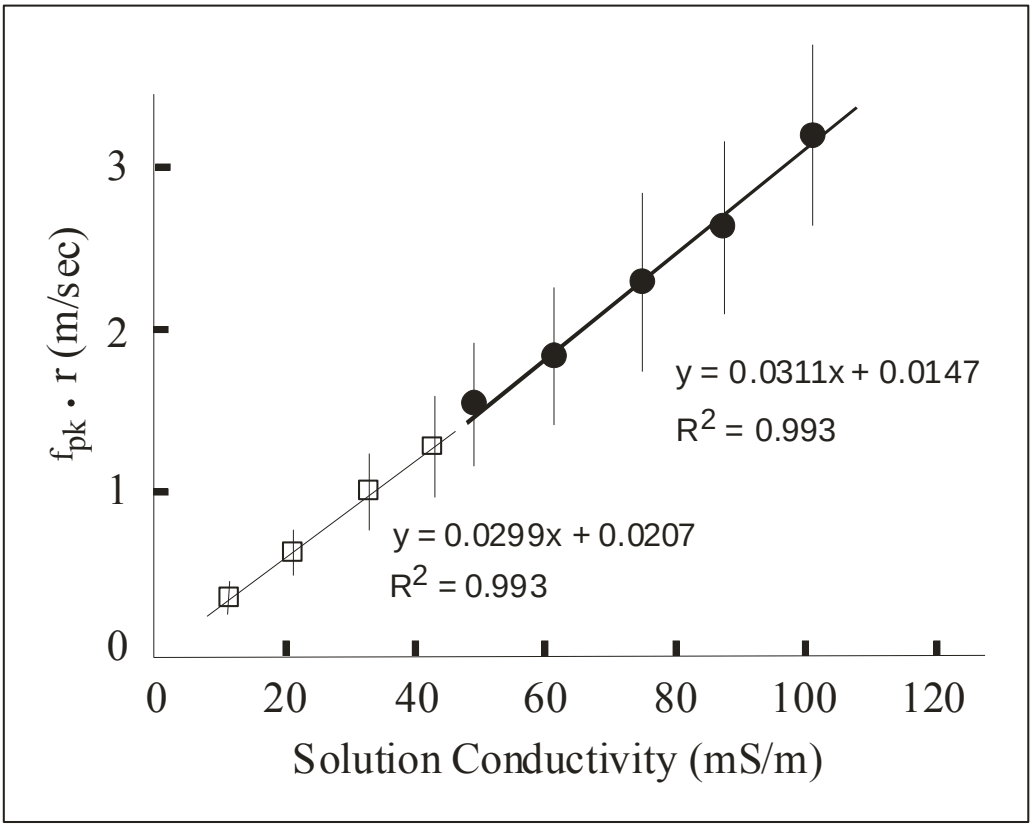

Figure 4